DOI: 10.1002/ejic.200700322

Sterically Demanding Iminopyridine Ligands

Torsten Irrgang,[a] Sandra Keller,[a] Heidi Maisel,[a] Winfried Kretschmer,[b] and Rhett Kempe*[a]

Keywords: Ethylene polymerization / N ligands / Cobalt / Iron / Nickel / Palladium

Two sterically demanding iminopyridine ligands, (2,6-diisopropylphenyl)[6-(2,4,6-triisopropylphenyl)pyridin-2-ylmethylene]amine and (2,6-diisopropylphenyl)[6-(2,6-dimethylphenyl)pyridin-2-ylmethylene]amine, were prepared by a two-step process: first, condensation of 6-bromopyridine-2-carbaldehyde with an equimolecular amount of 2,6-diisopropylaniline, and second, Kumada-type coupling of in-situ-formed Grignard compounds of 1-bromo-2,6-dimethylphenyl and 1-bromo-2,4,6-triisopropylphenyl. Dichlorido complexes of the ligands were synthesized starting from $FeCl_2$, $[PdCl_2(cod)]$, $[NiCl_2(dme)]$, and $CoCl_2$ (cod = 1,5-cyclooctadiene, dme = dimethoxyethane). X-ray crystal structure analyses of a Fe, Pd, and Co complex were determined. Ethylene polymerization/oligomerization behavior of the dichlorido complexes after activation with methylaluminoxane or triethylaluminum was studied. Ethylene dimerization selectivity greater than 95 % was observed.

Introduction

Olefin polymerization catalyzed by late-transition-metal complexes is an intensively explored area of research.[1] Out of the neutral N ligand environments studied so far, diimine group 10 (Scheme 1, left) and the pyridyl diimine Fe/Co catalysts (Scheme 1, right) have received most of the attention.[2] Remarkable changes in the polymerization behavior especially with regard to the obtained molecular weights of the polymers have been observed for these complexes if very bulky 2,6-diisopropylphenyl substituents were introduced.

Scheme 1. N-ligand-stabilized late-transition-metal olefin polymerization precatalysts (for instance: M = Ni, Pd; M′ = Fe, Co; X = Cl; R = H; $R^1 = CH_3$; Ar = 2,6-diisopropylphenyl).

Iminopyridine ligands (Scheme 2, right) might be considered to be structurally related to both of the above-mentioned ligand systems, and consequently, the olefin polymerization behavior of some of these complexes was investigated recently.[3–5] Sterically demanding examples bearing 2,6-diisopropylphenyl substituents in the pyridine ring are not known to the best of our knowledge.

[a] Lehrstuhl für Anorganische Chemie II, Universität Bayreuth, 95440 Bayreuth, Germany
E-mail: kempe@uni-bayreuth.de
[b] Stratingh Institut for Chemistry, Center for Catalytic Olefin Polymerization, University of Groningen, Nijenborgh 4, 9747 AG Groningen, The Netherlands

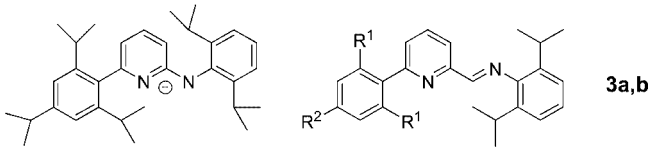

3a,b

Scheme 2. Sterically demanding aminopyridinato ligands (left) and iminopyridines [**3a**: $R^1 = CH_3$, R^2 = H; **3b**: $R^1 = R^2 = CH(CH_3)_2$].

Bianchini and coworkers for instance described phenyl and naphthalenyl substitution at the pyridine ring by Suzuki coupling.[4] It may not be possible to use such a protocol to cross couple sterically demanding phenyl derivatives like 2,6-diisopropylphenyl.[6] We recently described an efficient protocol to introduce 2,6-diisopropylphenyl substituents into pyridine rings by Kumada coupling. This chemistry was explored to synthesize sterically demanding aminopyridines[7] and to use them as aminopyridinato ligands (Scheme 2, left);[8] a class of ligands we investigated intensively in the past.[9]

Because of the importance of steric protection in late-metal-catalyzed olefin polymerization chemistry, as well as other areas of coordination chemistry, we became interested in the synthesis of bulky iminopyridines such as **3a**,**b** (Scheme 2, right). We felt that an approach we used to synthesize bulky aminopyridines might by suitable for the synthesis of ligands such as **3a**,**b** as well. The imine function that is usually sensitive towards the addition of Grignard reagents might be well enough protected due to the 2,6-diisopropylphenyl substituent at the imine N atom. Herein we report the synthesis of sterically demanding iminopyridine ligands, the syntheses and structures of Co, Ni, Fe,

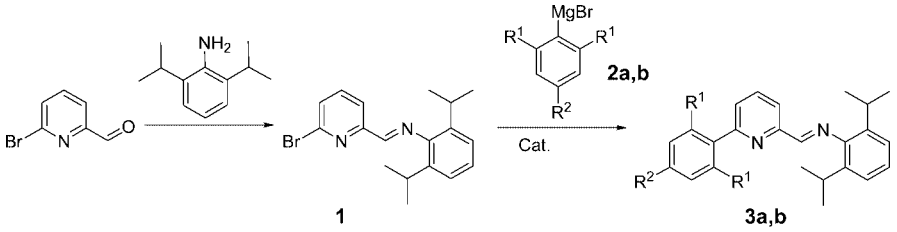

Scheme 3. Synthesis of **3** [R^1 = CH_3, R^2 = H (**2a/3a**); R^1 = R^2 = *i*Pr (**2b/3b**); cat for Kumada coupling is $FeCl_2$ or $MnCl_2$].

and Pd complexes stabilized by these ligands, and some aspects of the olefin polymerization/oligomerization behaviors of a few of these complexes.

Results and Discussion

Syntheses of the Ligands

The sterically demanding iminopyridine ligands **3a**,**b**[10] were prepared by the two-step process illustrated in Scheme 3. First, the convenient condensation of 6-bromopyridine-2-carbaldehyde with an equimolecular amount of 2,6-diisopropylaniline leads to **1**.[11] The reaction of in-situ-formed Grignard compounds **2a**,**b** of 1-bromo-2,6-dimethylphenyl and 1-bromo-2,4,6-triisopropylphenyl with **1** in the presence of a catalytic amount of $FeCl_2$ leads to iminopyridines **3a**,**b** (Scheme 3).[12] We observed similar results by using $MnCl_2$ as a catalyst. The catalyst was chosen on the basis of the results that were obtained from screening experiments with various transition-metal halogenides and N or P ligands. The 2,6-diisopropylphenyl group at the imine N atom protects the imine well enough if an efficient catalyst is added to accomplish biaryl formation.

Compounds **3a**,**b** were obtained as pale yellow crystalline materials. They differ in the steric demand (R^1 and R^2) of the phenyl substituent in the 6-position of the pyridine ring.

Syntheses and Structures of the Complexes

Complexes **4**–**7** were obtained in high yields in the reaction of 1 equiv. of **3a** with anhydrous $FeCl_2$, [$PdCl_2$(cod)], [$NiCl_2$(dme)], and $CoCl_2$ (cod = 1,5-cyclooctadiene, dme = dimethoxyethane) in thf at 70 °C for 18 h (Scheme 4).

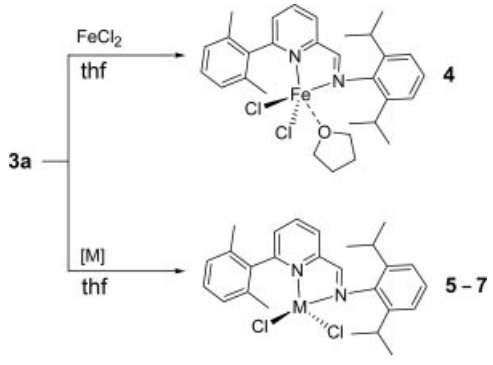

Scheme 4. Reaction of **3a** with late-transition-metal halogenides {[M] = [$PdCl_2$(cod)] (**5**); [$NiCl_2$(dme)] (**6**); $CoCl_2$ (**7**)}.

Single crystals of red paramagnetic complex **4** and yellow crystals of diamagnetic **5**[13] were grown from a concentrated thf solution at –25 °C. For both complexes, one uncoordinated thf molecule was found in the crystal lattice, and for **4**, one additional coordinated thf ligand was found. ORTEP drawings are reported in Figures 1 and 2 for **4** and **5**, respectively. Crystallographic details are summarized in Table 2. In **4**, the iron is five coordinate, and the coordination sphere is best described as distorted trigonal bipyramidal with the equatorial plane being occupied by the imino N atom and the two chlorine atoms. The axial positions are coordinated by the pyridine N atom and by the O atom of the coordinated thf ligand. A Cl–Fe–Cl angle of 131.81(6)° is observed within the equatorial plane and a "chelating" angle $N_{pyridine}$–Fe–N_{imino} of 77.30(16)°. The Fe–O bond of the coordinated thf ligand is rather long [2.474(8) Å], which indicates a very weakly bound thf ligand. The Fe–O bond lengths of thf-coordinated iron chlorides range from 1.944 Å for [$FeCl_3$(thf)][14] to 2.181 Å for the [Fe_2Cl_3-$(thf)_6$]$^-$ anion.[15] The coordination of **5** is best described as square planar with a $N_{pyridine}$–Pd–N_{imino} angle of 80.50(15)° and Cl–Pd–Cl angle of 88.84(5)°.

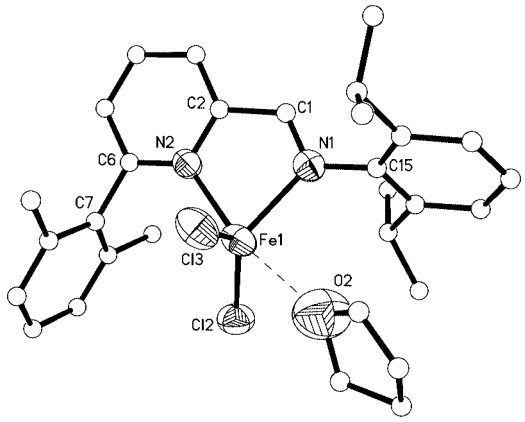

Figure 1. Molecular structure of **4**; selected bond lengths [Å] and angles [°]: C1–N1 1.271(6), C1–C2 1.486(7), C2–N2 1.357(6), C6–N2 1.353(6), C6–C7 1.490(7), C15–N1 1.441(6), N1–Fe1 2.140(4), N2–Fe1 2.201(4), Cl2–Fe1 2.2369(17), Cl3–Fe1 2.2586(17), O2–Fe1 2.473; N1–C1–C2 120.3(5), N2–C2–C1 115.4(5), N2–C6–C7 118.1(4), C1–N1–C15 118.4(4), C1–N1–Fe1 113.9(3), C15–N1–Fe1 126.9(3), C6–N2–C2 117.1(4), C6–N2–Fe1 131.0(3), C2–N2–Fe1 111.3(3), N1–Fe1–N2 77.30(16), N1–Fe1–Cl2 122.05(12), N2–Fe1–Cl2 105.29(12), N1–Fe1–Cl3 103.30(12), N2–Fe1–Cl3 99.34(12), Cl2–Fe1–Cl3 131.81(6).

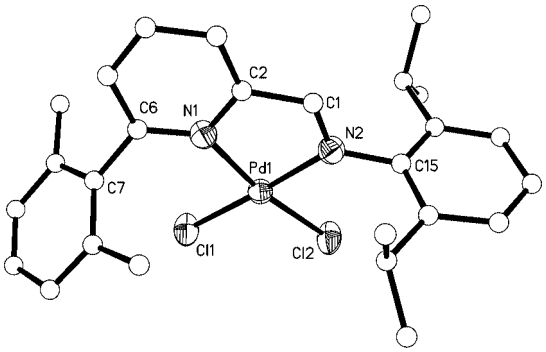

Figure 2. Molecular structure of **5**; selected bond lengths [Å] and angles [°]: Pd1–N2 2.012(4), Pd1–N1 2.090(4), Pd1–Cl1 2.273(13), Pd1–Cl2 2.2746(15), N2–C1 1.272(6), N2–C15 1.464(6), N1–C6 1.347(6), N1–C2 1.355(6), C1–C2 1.451(6), C6–C7 1.489(8); N2–Pd1–N1 80.50(15), N2–Pd1–Cl1 176.40(13), N1–Pd1–Cl1 99.43(10), N2–Pd1–Cl2 91.01(12), N1–Pd1–Cl2 170.89(11), Cl1–Pd1–Cl2 88.84(5), C1–N2–C15 117.9(4), C1–N2–Pd1 113.8(3), C15–N2–Pd1 128.2(3), C6–N1–C2 117.1(4), C6–N1–Pd1 132.8(3), C2–N1–Pd1 110.0(3), N2–C1–C2 119.1(4), N1–C2–C1 115.3(4), N1–C6–C7 121.2(4).

The reaction of sterically more demanding ligand **3b** with the anhydrous metal salts $FeCl_2$, $[PdCl_2(cod)]$, $[NiCl_2(dme)]$, and $CoCl_2$ leads to corresponding complexes **8**–**11** (Scheme 5). Compounds **8**, **10**, and **11** are paramagnetic.

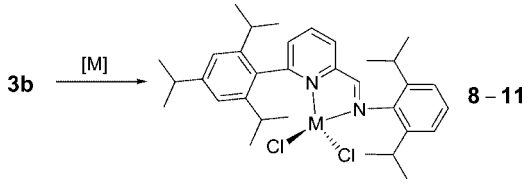

Scheme 5. Synthesis of **8** (M = Fe), **9** (M = Pd), **10** (M = Ni), and **11** (M = Co).

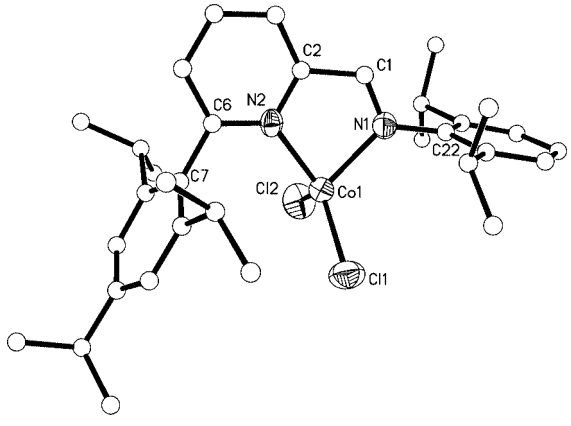

Figure 3. Molecular structure of **11**; selected bond lengths [Å] and angles [°]: Co1–N2 2.052(4), Co1–N1 2.057(4), Co1–Cl2 2.2023(16), Co1–Cl1 2.2007(15), N2–C2 1.346(6), N2–C6 1.353(6), N1–C1 1.267(6), N1–C22 1.453(6), C1–C2 1.477(7), C6–C7 1.479(7); N2–Co1–N1 80.23(16), N2–Co1–Cl2 111.01(11), N1–Co1–Cl2 109.89(12), N2–Co1–Cl1 125.20(12), N1–Co1–Cl1 113.17(22), Cl2–Co1–Cl1 112.60(7), C2–N2–C6 118.6(4), C2–N2–Co1 112.3(3), C6–N2–Co1 128.8(3), C1–N1–C22 120.1(4), C1–N1–Co1 113.2(3), C22–N1–Co1 126.7(3), N1–C1–C2 118.6(4), N2–C2–C1 114.7(4), N2–C6–C7 118.6(4).

The coordination of the cobalt centre of **11** is best described as slightly distorted tetrahedral. For the three structurally characterized metal complexes we observed three different coordination environments. The sterically demanding N ligands introduced here seem to be quite flexible with regard to the coordination they adopt with transition metals, and they do not force metals in energetically unfavored coordinations because of steric pressure. The chelating $N_{pyridine}$–Co–N_{imino} angle of **11** is 80.24°. The bulky phenyl substituents in the 6-position of the pyridine and at the imino N atom are twisted relative to the pyridine ring with dihedral angles of 99.8° and 97.1°, respectively. The five-membered chelating C_2CoN_2 ring is nearly planar (0.0473 Å mean deviation). Details of the X-ray crystal structure analysis of **11** are summarized in Table 2. The molecular structure of **11** is shown in Figure 3.

Olefin Polymerization/Oligomerization Behavior

Oligomerization results are summarized in Table 1. The investigated complexes mainly produce oligomeric materials. Nearly no activity is observed for the iron complexes. The highest activities are observed for the cobalt and nickel complexes. For both metals, Co and Ni, the changes in terms of activity and distribution of the oligomers are rather small. The sterically more demanding ligand shows essentially the same polymerization behavior, aside from a little enhanced activity. Noteworthy is that the selectivity for **6**, **7**, **10**, and **11** towards 1-butene is high. High ethylene dimerization selectivities were observed for iminopyridine complexes bearing sterically less-demanding substituents on the pyridine ring as well.[4] Activation with triethylaluminum (TEA), Et_3Al, instead of methylaluminoxane (MAO), leads to reduced activity but suppresses the formation of polymeric byproducts and increases the dimerization selectivity above 95%. The results obtained with our Co complexes are similar to (or nearly as good as) the results observed by Bianchini and coworkers.[4] They observed for iminopyridine Co complexes (activated with MAO) carrying a phenyl or naphthyl substituent on the pyridine ring the formation of oligomerization products and butenes, especially with conversions of 784 and 630 $kg_{product}mol_{cat}^{-1}h^{-1}bar^{-1}$, respectively. This comparison indicates that the introduction of steric bulk in the 6-position of the pyridine ring does not influence the nature of the products formed. It was recently demonstrated by these groups that their tetrahedral high-spin complexes react with MAO in toluene to give low-spin Co square-planar methyl complexes.[4e] This species, intercepted by EPR spectroscopy, inserts ethylene to form a cobalt–propyl intermediate that eliminates propene with the formation of a Co–H initiator. A similar mechanism is most likely in operation for our Co (and Ni) complexes; by ethylene insertion into a Co–H bond, an ethyl complex is formed. If this species undergoes β-H elimination/transfer we get back to the starting point (Co–H complex and ethylene). If a second insertion of ethylene takes place, a butyl complex is formed and

Table 1. Ethylene polymerization/oligomerization of metal complexes by using different activation protocols.[a] Products were analyzed by GC with the use of α-olefins as internal standards.

Run	Complex[b]	Activator[c]	Conversion [$kg\,mol_{cat}^{-1}\,h^{-1}\,bar^{-1}$]	$m_{Pol.}$ [g]	C-4[d] [g]	C-6 [g]	C-8 [g]	Higher [g]
1	**4**, Fe	MAO	2	0.05	–	–	–	–
2	**4**, Fe[e]	TEA	0	–	–	–	–	–
3	**8**, Fe*	MAO	2	0.06	–	–	–	–
4	**8**, Fe*[e]	TEA	0	–	–	–	–	–
5	**7**, Co	MAO	358	0.06	3.95	0.55	–	–
6	**7**, Co[e]	TEA	152	–	1.85	0.05	–	–
7	**11**, Co*	MAO	472	0.06	5.00	0.80	–	–
8	**11**, Co*[e]	TEA	172	–	2.10	0.05		
9	**6**, Ni	MAO	150	0.06	1.16	0.35	0.23	0.11
10	**6**, Ni	MMAO-3A	136	0.06	1.10	0.15	nd[f]	nd[f]
11	**10**, Ni*	MAO	156	0.06	1.27	0.59	0.03	–
12	**10**, Ni*	MMAO-3A	140	0.06	1.21	0.34	nd[f]	nd[f]
13	**5**, Pd	MAO	12	0.3	–	–	–	–
14	**5**, Pd	MMAO-3A	8	0.2	–	–	–	–
15	**9**, Pd*	MAO	20	0.5	–	–	–	–
16	**9**, Pd*	MMAO-3A	12	0.3	–	–	–	–

[a] The general procedure and conditions as described in the Experimental Section were followed by using the catalyst (10 μmol), the activator (500 equiv.), and toluene (260 mL) at 30 °C, 5 bar ethylene with a 15 min run time. [b] * Indicates the sterically more-demanding ligand. [c] MMAO-3A: Modified MAO $\{[Me_{0.7}iBu_{0.3}AlO]_n\}$. [d] >95% 1-Butene. [e] M/Al, 1:200. [f] Not determined, isoparaffinic solvent (b.p. 118 °C).

subsequently butene can be eliminated. It looks as though β-H elimination/transfer is very fast with regard to chain growth for our Co complexes and thus we preferentially obtain butenes. If we activate with TEA, β-H elimination/transfer may become enhanced because butene selectivity is increased. Alternatively, TEA may reduce the Co dichloride complexes followed by oxidative coupling of two ethylene molecules including the formation of a cobaltacyclopentene followed by β-H elimination, forming a butenyl hydride that undergoes reductive elimination, and butene is formed. The stability of the transient cobaltacyclopropene against further ethylene insertion may lead to the exclusive formation of the dimerization product. Interestingly, we are able to dimerize selectively with relatively low cocatalyst loadings and MAO was not needed. Mapolie and coworkers studied the formation of polymeric materials for Pd complexes.[5] Conversions up to 15 $kg_{product}\,mol_{cat}^{-1}\,h^{-1}\,bar^{-1}$ were observed, which again is in accordance with the results obtained for our Pd complexes. Once more, no dramatic influence is seen due to the introduction of the very bulky substituents on the pyridine ring. It is surprising that the electronic situation that the iminopyridines provide dominate the polymerization chemistry and that the bulkiness of the ligands on the pyridine ring is of minor relevance despite the difference in shielding at the metal center. The shielding is visualized in Figure 4.

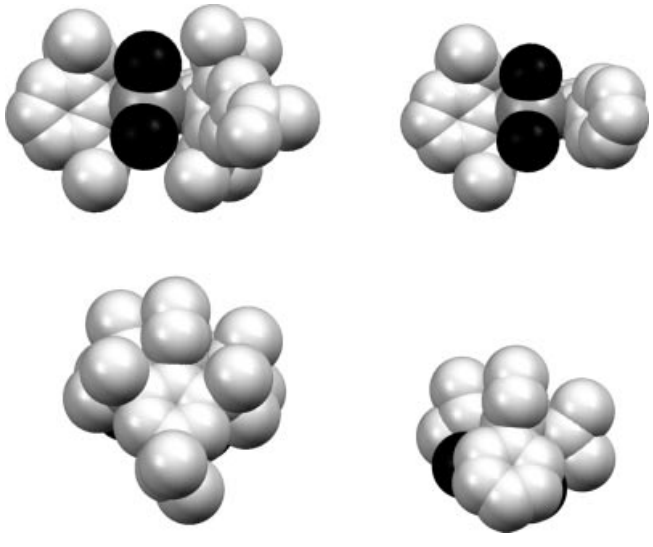

Figure 4. Visualization (space filling plot with C atoms light grey, Co atoms dark grey, Cl atoms black) of the steric protection of the 2,4,6-triisopropylphenyl substituent at the pyridine ring (right) versus shielding provided by a phenyl ring only (left).

Conclusions

Four general conclusions can be drawn from the investigations discussed here. First, Kumada coupling is an efficient protocol to introduce sterically demanding substituents in the 6-position of the pyridyl ring of iminopyridines. Second, the sterically demanding ligands discussed here accomplish a variety of coordinations with late transition metals, such as trigonal bipyramidal, tetrahedral, and square planar. Third, the cobalt and nickel dichlorido complexes (if activated with MAO or TEA) dimerize ethylene rather than polymerize it and can show dimerization selectivities greater than 95%. Fourth, the introduction of the bulky 2,6-dialkylphenyl substituent in the pyridine moiety does not influence the polymerization behavior of the resulting late-transition-metal complexes (activation with MAO) tremendously relative to the significantly less bulky versions of those ligands.

Experimental Section

Polymerization Experiments

General: Toluene (Aldrich, anhydrous, 99.8%) was passed over columns of Al_2O_3 (Fluka), BASF R3–11 supported Cu oxygen scavenger and molecular sieves (Aldrich, 4 Å) prior to use. Ethylene (AGA polymer grade) was passed over BASF R3–11 supported Cu oxygen scavenger and molecular sieves (Aldrich, 4 Å) prior to use. TEA (1.6 M in toluene, Aldrich), PMAO (4.9 wt.-% in Al, toluene, Akzo), and MMAO-3A (2.1 wt.-% in Al; isoparaffinic solvent, b.p. 118 °C; Akzo) were used as received.

Preparative Procedure: The polymer samples were prepared by dissolving the polymer (15 mg) in CD_2Cl_2 (0.5 mL) at 100 °C for 3 h before measuring. Gel permeation chromatography (GPC) analysis was carried out with a Polymer Laboratories Ltd. (PL-GPC210) chromatograph, equipped with a capillary differential viscometer (Viscotek), a refractive index (RI) detector, and a two-angle (15 and 90°) light-scattering photometer at 150 °C by using 1,2,4-trichlorobenzene as the mobile phase. The samples were prepared by dissolving the polymer (0.1% weight/volume) in the mobile phase solvent in an external oven and were run without filtration. The molecular weight was referenced to polyethylene (M_w = 50000 g mol^{-1}) and polystyrene (M_w = 100000–500000 g mol^{-1}) standards. The reported values are the average of at least two independent determinations. GC analyses were performed with an HP 6890 instrument equipped with an HP-1 dimethylpolysiloxane column (19095 Z-123). GC–MS analyses were conducted with an HP 5973 mass-selective detector attached to an HP 6890 GC instrument.

Polymethylaluminoxane (PMAO) Ethylene Conversion: The catalytic ethylene conversion reactions were performed in a stainless steel 1-L autoclave (Medimex) in the semibatch mode (ethylene was added by replenishing flow to keep the pressure constant). The reactor was temperature, flow, and pressure controlled and equipped with separated toluene, catalyst, and cocatalyst injection systems and a sample outlet for continuous reaction monitoring. Up to 15 bar of ethylene pressure multiple injections of the catalyst with a pneumatically operated catalyst injection system were used. During a polymerization run, the pressure, the ethylene flow, the inner and the outer reactor temperature, and the stirrer speed were monitored continuously. In a typical semibatch experiment, the autoclave was evacuated and heated for 1 h at 125 °C prior to use. The reactor was then brought to the desired temperature, stirred at 600 rpm and charged with toluene (230 mL), PMAO (2.7 g of a toluene solution, 4.9 wt.-% Al, 5 mmol), and cyclohexane (10 g) as an internal standard. After pressurizing with ethylene to reach a total pressure of 5 bar, the autoclave was equilibrated for 5 min. Subsequently, the catalyst (10 μmol, M/Al, 1:500) suspended in toluene (30 mL) was injected to start the reaction. During the run the ethylene pressure was kept constant to within 0.2 bar of the initial pressure by replenishing flow. After a reaction time of 15 min, a sample of the reaction mixture was taken to analyze and quantify the soluble products before the reactor was vented and the residual aluminum alkyls were destroyed by the addition of ethanol (100 mL). The polymeric product was collected, stirred for 30 min in acidified ethanol, and rinsed with ethanol and acetone on a glass frit. The polymer was initially dried in air and subsequently in vacuo at 80 °C. The results are presented in Table 1.

MMAO-3A Ethylene Conversion: The general procedure and conditions as described above were followed with the use of MMAO-3A (6.4 g of an isoparaffinic solvent, b.p. 118 °C; 2.1 wt.-% Al, 5 mmol, M/Al, 1:500) instead of PMAO to charge the reactor. The results are presented in Table 1.

TEA Ethylene Conversion: The general procedure and conditions as described above were followed with the use of TEA (M/Al, 1:200) instead of PMAO to charge the reactor. The results are presented in Table 1.

Syntheses and Structure Analyses

General: All reactions and manipulations with air-sensitive compounds were performed under an atmosphere of dry argon by using standard Schlenk and glove box techniques. Nonhalogenated solvents were distilled from sodium benzophenone ketyl and halogenated solvents from P_2O_5. Deuterated solvents were obtained from Cambridge Isotope Laboratories and were degassed, dried, and distilled prior to use. All other chemicals were purchased from commercial vendors and used without further purification. NMR spectra were obtained with a Bruker ARX 250 spectrometer. Chemical shifts are reported in ppm relative to the deuterated solvent. Elemental analyses were carried out with a Vario elementar EL III. Melting points were measured in sealed capillaries with a Stuart SMP3 apparatus. Magnetic moments were determined with a magnetic susceptibility balance Sherwood Mark 1 MSB at room temperature. X-ray crystal structure analyses were performed by with a STOE-IPDS II equipped with an Oxford Cryostream low-temperature unit. Structure solution and refinement were accomplished by using SIR97,[16] SHELXL-97,[17] and WinGX.[18] Crystallographic details are summarized in Table 2. CCDC-639686 (for **4**), -639684 (for **5**), and -639685 (for **11**) contain the supplementary crystallographic data for this publication. These data can be obtained free of charge from The Cambridge Crystallographic Data Centre via www.ccdc.cam.ac.uk/data_request/cif.

Syntheses of the Ligands and Ligand Precursors

1: 6-Bromopyridine-2-carbaldehyde (2.0 g, 10.7 mmol) and 2,6-diisopropylaniline (2.03 mL, 1.91 g, 10.7 mmol) were dissolved in ethanol (30 mL), and the mixture was heated at reflux for 2 h. The solvent was removed under reduced pressure, and a pale yellow crystalline material was obtained and used without further purification. Yield: 3.59 (97%). M.p. 104 °C. ^{1}H NMR (250.13 MHz, $CDCl_3$): δ = 8.26–8.25 (d, J = 1.0 Hz, 1 H, CH), 8.23 (s, 1 H, N=CH), 7.73–7.66 (t, J = 7.8 Hz, 1 H, CH), 7.61–7.57 (dd, J = 7.9, 1.0 Hz, 1 H, CH), 7.24–7.08 (m, 3 H, CH), 3.08–2.92 [sept, J = 6.9 Hz, 2 H, 2 × CH(CH$_3$)$_2$], 1.16–1.13 [d, J = 6.9 Hz, 12 H, 2 × CH(CH_3)$_2$] ppm. ^{13}C NMR (62.90 MHz, $CDCl_3$): δ = 161.44 (N=CH), 155.40, 147.85, 141.81, 138.99, 136.99, 129.79, 124.66, 123.03 (C$_m$, C$_6$H$_3$), 119.86, 27.91 [2 × CH(CH$_3$)$_2$], 23.37 [2 × CH(CH$_3$)$_2$] ppm. $C_{18}H_{21}BrN_2$ (345.28): calcd. C 62.61, H 6.13, N 8.11; found C 62.66, H 6.05, N 8.01.

2a: A solution of 2-bromo-*m*-xylene (1.39 mL, 1.93 g, 10.4 mmol) in thf (30 mL) was added to magnesium turnings (0.30 g, 12.5 mmol), and the resulting suspension was stirred and activated by the addition of 1,2-bromoethane (0.2 mL). An exothermic reaction took place, and an ice bath was used to cool the reaction mixture when the reaction became too vigorous. The reaction mixture was stirred at r.t. for 2 h and then filtered, and the filtrate was directly used.

2b: To a suspension of magnesium turnings (0.21 g, 8.69 mmol) in thf (100 mL) was added by syringe 1-bromo-2,4,6-triisopropylbenzol (1.82 mL, 7.24 mmol). The resulting suspension was stirred and activated by the addition of 1,2-bromoethane (0.2 mL). A low exothermic reaction took place. The reaction mixture was stirred at r.t. for 2 h and then filtered, and the filtrate was directly used.

3a: To a solution of **1** (3.0 g, 8.69 mmol) in dioxane (30 mL) was added a suspension of $FeCl_2$ (0.11 g, 0.87 mmol) in thf (10 mL). The Grignard solution **2a** was then slowly added to the stirred sus-

Table 2. Details of the X-ray crystal structure analyses of **4**, **5**, and **11**.

	4	**5**	**11**
Formula	$C_{34}H_{46}Cl_2FeN_2O_2$	$C_{30}H_{38}Cl_2N_2OPd$	$C_{45}H_{68}Cl_2CoN_2O_3$
M [g mol^{-1}]	641.48	619.92	814.84
Crystal system	monoclinic	monoclinic	hexagonal
Space group	$P2_1/c$	$P2_1/c$	$P6_1$
a [Å]	17.386(1)	9.428(1)	13.013(1)
b [Å]	13.495(1)	13.677(2)	13.013(1)
c [Å]	14.802(1)	23.309(2)	47.354(4)
β [°]	96.69(1)	93.82(1)	
V [Å^3]	3449.3(4)	2999(1)	6944.5(1)
Z	4	4	6
Crystal size [mm]	$0.86 \times 0.10 \times 0.05$	$0.33 \times 0.15 \times 0.05$	$0.32 \times 0.12 \times 0.11$
$\rho_{calcd.}$ [g cm^{-3}]	1.235	1.373	1.169
Absorption correction	numerical	no	no
T [K]	193(2)	193(2)	193(2)
θ range [°]	1.92–26.27	1.73–25.64	1.81–21.86
Reflections collected	45992	12594	52889
Independent reflections	6890	5400	5542
Observed reflections	3082	3630	4716
R value [$I > 2\sigma(I)$]	0.0695	0.0481	0.0475
wR_2 (all data)	0.2061	0.0951	0.1183

pension. The reaction mixture was heated to 70 °C for 48 h. Water (100 mL) and diethyl ether (80 mL) were added, and the resulting suspension was transferred to a 500-mL separatory funnel. The organic phase was collected, and the inorganic phase was washed twice with diethyl ether and extracted. The combined organic phases were washed with a saturated NaCl solution and dried with Na_2SO_4. The organic phase was concentrated to dryness under vacuum, resulting in a brown oily product. The oil was purified by silica chromatography (pentane) and then crystallized from pentane at –25 °C to afford a pale yellow crystalline material. Yield: 1.16 g (39%). M.p. 142.5 °C. ^{1}H NMR (250.13 MHz, $CDCl_3$): δ = 8.36 (s, 1 H, N=CH), 8.29–8.25 (dd, J = 7.9, 1.1 Hz, 1 H, pyridine), 7.95–7.89 (t, J = 7.7 Hz, 1 H, $4_{pyridine\text{-}H}$), 7.37–7.34 (dd, J = 7.6, 1.1 Hz, 1 H, pyridine), 7.25–7.04 (m, 6 H, $2 \times C_6H_3$), 3.08–2.92 [sept, J = 6.9 Hz, 2 H, $2 \times CH(CH_3)_2$], 2.12 (s, 6 H, $2 \times CH_3$), 1.20–1.17 [d, J = 6.9 Hz, 12 H, $2 \times CH(CH_3)_2$] ppm. ^{13}C NMR (62.90 MHz, $CDCl_3$): δ = 163.29 (N=CH), 159.76 (C), 154.31 (C), 148.35 (C), 139.73 (C), 137.13 ($2 \times$ C), 137.01 (CH), 135.84 ($2 \times$ C), 128.17 (CH), 127.79 ($2 \times$ CH), 126.21 (CH), 124.35 (CH), 122.96 ($2 \times$ CH), 119.08 (CH), 27.90 [$2 \times CH(CH_3)_2$], 23.41 [$2 \times$ CH-$(CH_3)_2$], 20.34 ($2 \times CH_3$) ppm. $C_{26}H_{30}N_2$ (370.54): calcd. C 84.28, H 8.16, N 7.56; found C 83.74, H 8.15, N 7.47.

3b: To a solution of **1** (2.5 g, 7.24 mmol) in dioxane (30 mL) at 70 °C was added a suspension of $FeCl_2$ (0.092 g, 0.72 mmol) in thf (30 mL). The Grignard solution **2b** was then slowly added to the stirred suspension. The reaction mixture was stirred at 70 °C for 48 h. Water (100 mL) and hexane (80 mL) were added, and the resulting suspension was transferred to a 500-mL separatory funnel. The organic phase was collected, and the inorganic phase was washed twice with hexane and extracted. The combined organic phases were washed with a saturated NaCl solution and dried with Na_2SO_4. The organic phase was concentrated under vacuum, and at –25 °C pale yellow crystals were obtained. Yield: 2.14 g (86%). M.p. 193.5 °C. ^{1}H NMR (250.13 MHz, $CDCl_3$): δ = 8.33 (s, 1 H, N=CH), 8.29–8.26 (dd, J = 7.8, 0.9 Hz, 1 H, pyridine), 7.92–7.86 (t, J = 7.7 Hz, 1 H, $4_{pyridine\text{-}H}$), 7.44–7.40 (dd, J = 7.6, 0.9 Hz, 1 H, pyridine), 7.19–7.10 (m, 5 H, C_6H_2/C_6H_3), 3.07–2.90 [sept, J = 6.8 Hz, 3 H, $3 \times (CH_3)_2CH\text{-}C_6H_2$], 2.63–2.46 [sept, J = 6.8 Hz, 2 H, $2 \times (CH_3)_2CH\text{-}C_6H_3$], 1.28–1.26 [d, J = 7.0 Hz, 12 H, $2 \times (CH_3)_2$-CH-C_6H_3], 1.18–1.12 [q, J = 6.8 Hz, 18 H, $3 \times (CH_3)_2CH\text{-}C_6H_2$] ppm. ^{13}C NMR (62.90 MHz, $CDCl_3$): δ = 163.61 (N=CH), 160.07 (C), 153.93 (C), 149.05 (C), 148.43 (C), 146.24 ($2 \times$ C), 137.22 ($2 \times$ C), 136.34 (CH), 135.71 (C), 126.60 (CH), 124.35 (CH), 122.99 ($2 \times$ CH), 120.96 ($2 \times$ CH), 118.87 (CH), 34.45 (CH), 30.48 (CH), 27.92 [$2 \times (CH_3)_2CH\text{-}C_6H_3$], 24.26 (CH), 24.09 (CH), 24.00 (CH), 23.49 [$2 \times (CH_3)_2CH\text{-}C_6H_3$] ppm. $C_{33}H_{44}N_2$ (468.72): calcd. C 84.56, H 9.46, N 5.46; found C 84.38, H 9.49, N 6.21.

Syntheses of the Complexes

4: A solution of **3a** (0.358 g, 0.97 mmol) and $FeCl_2$ (0.11 g, 0.86 mmol) in thf (30 mL) was heated at 70 °C whilst stirring for 18 h. The solvent was removed under vacuum, and the red residue was washed with hexane, dissolved in thf, and filtered through quartz. The filtrate was concentrated, and red crystals were grown at –25 °C. Yield: 0.434 g (90%). M.p. 240 °C. μ_{eff} = 4.44 BM (24.4 °C). ^{1}H NMR (250.13 MHz, $CDCl_3$): δ = 34.50, 30.98, 8.23, 7.63, 7.14, 5.90, 3.97, 2.89, 2.03, 1.74, 1.23, 1.14, 0.86, 0.05, –2.57 ppm. $C_{26}H_{30}Cl_2FeN_2$ (497.25): calcd. C 62.80, H 6.08, N 5.63; found C 63.26, H 6.05, N 5.24.

5: A stirred solution of **3a** (0.229 g, 0.81 mmol) and [$PdCl_2$(cod)] (0.223 g, 0.79 mmol) in thf (30 mL) was heated at 70 °C for 18 h. The solvent was removed under vacuum, and the residue was washed with hexane, dissolved in dichloromethane (50 mL), and filtered through quartz. The resulting orange solution was concentrated, and yellow-orange crystals (needles) were grown at –25 °C. Yield: 76%. M.p. 255 °C. ^{1}H NMR (250.13 MHz, CD_2Cl_2): δ = 8.23–8.16 (t, J = 7.5 Hz, 1 H, $4_{pyridine\text{-}H}$), 8.19 (s, 1 H, N=CH), 7.97–7.94 (dd, J = 7.7, 1.5 Hz, 1 H, pyridine), 7.59–7.55 (dd, J = 8.3, 1.5 Hz, 1 H, pyridine), 7.40–7.09 (m, 6 H, $2 \times C_6H_3$), 3.44–3.31 [sept, J = 6.8 Hz, 2 H, $2 \times CH(CH_3)_2$], 2.30 (s, 6 H, $2 \times CH_3$), 1.40–1.37 (d, J = 6.8 Hz, 6 H, $2 \times CH_3$, isopropyl), 1.19–1.16 (d, J = 6.9 Hz, 6 H, $2 \times CH_3$, isopropyl) ppm. ^{13}C NMR (62.90 MHz, CD_2Cl_2): δ = 170.22 (N=CH), 166.21 (C), 154.87 (C), 143.30 (C), 140.98 (C), 140.11 (CH), 138.40 (C), 135.93 (CH), 133.78 (CH), 129.55 (CH), 128.76 (CH), 127.59 (CH), 123.49 (CH), 28.97 [$2 \times CH(CH_3)_2$], 24.27 ($2 \times CH_3$, isopropyl), 22.93 ($2 \times CH_3$, isopropyl), 20.68 [$(CH_3)_2CH\text{-}C_6H_4$] ppm. $C_{26}H_{30}Cl_2N_2Pd \cdot 0.5CH_2Cl_2$ (590.29): calcd. C 53.92, H 5.29, N 4.75; found C 53.52, H 5.35, N 4.41.

6: Compound **3a** (0.25 g, 0.67 mmol), [$NiCl_2$(dme)] (0.145 g, 0.66 mmol), and thf (50 mL) were added together in a Schlenk flask under an atmosphere of nitrogen. The reaction mixture was stirred at 70 °C for 18 h. The solvent was removed under vacuum, and the red residue was washed with hexane, dissolved in thf, and filtered through quartz. The filtrate was concentrated, and orange crystals were grown at –25 °C. Yield: 0.256 g (59%). μ_{eff} = 2.99 BM (25.9 °C). ^{1}H NMR (250.13 MHz, $CDCl_3$): δ = 32.03, 24.09, 20.65, 10.74, 8.85, 8.34, 8.24, 7.92, 7.14, 5.48, 3.75, 2.99, 2.41, 2.10, 1.85, 1.18, 0.89, 0.06 ppm. $C_{26}H_{30}Cl_2N_2Ni{\cdot}2C_4H_8O$ (644.34): calcd. C 63.38, H 7.20, N 4.35; found C 63.04, H 7.57, N 4.54.

7: In a closed Schlenk flask, a stirred solution of **3a** (0.362 g, 0.98 mmol) and $CoCl_2$ (0.12 g, 0.92 mmol) in thf (30 mL) was heated at 70 °C for 18 h. The solvent was removed under vacuum, and the red residue was washed with hexane, dissolved in thf, and filtered through quartz. The filtrate was concentrated, and green needles were grown at –25 °C. Yield: 0.43 g (77%). M.p. 300 °C. μ_{eff} = 4.17 BM (25.9 °C). ^{1}H NMR (250.13 MHz, $CDCl_3$): δ = 34.70, 32.45, 19.13, 7.16, 5.21, 3.75, 3.34, 2.33, 2.15, 2.09, 1.80, 1.43, 1.22, 1.17, 1.14, 1.10, 0.85, 0.82, 0.04, –2.40, –3.37, –8.80 ppm. $C_{26}H_{30}Cl_2CoN_2{\cdot}C_4H_8O$ (572.47): calcd. C 62.94, H 6.69, N 4.89; found C 63.23, H 6.22, N 5.18.

8: In a dry box, **3b** (0.243 g, 0.52 mmol), $FeCl_2$ (0.066 g, 0.52 mmol), and thf (50 mL) were combined in a Schlenk flask under an atmosphere of nitrogen. The resulting solution was stirred at 60 °C for 48 h. The solvent was removed, and the precipitate was washed with hexane, dissolved in thf, and filtered through quartz. The filtrate was concentrated to dryness under vacuum, resulting in a dark red solid product. Yield: 0.11 g (32%). μ_{eff} = 6.16 BM (25.1 °C). ^{1}H NMR (250.13 MHz, $CDCl_3$): δ = 39.31, 8.23, 7.86, 7.09, 2.92, 2.50, 1.56, 1.13, 0.05 ppm. $C_{33}H_{44}Cl_2FeN_2{\cdot}C_4H_8O$ (667.57): calcd. C 66.57, H 7.85, N 4.20; found C 66.38, H 7.55, N 3.92.

9: A stirred solution of **3b** (0.252 g, 0.538 mmol) and [$PdCl_2$(cod)] (0.138 g, 0.483 mmol) in thf (50 mL) was heated at 60 °C for 72 h. The solvent was removed under vacuum, and the residue was washed with hexane, dissolved in toluene (50 mL), and filtered through quartz. The solvent was then removed, and the yellow product was dried under vacuum. Yield: 0.18 g (47%). M.p. 161 °C. ^{1}H NMR (250.13 MHz, CD_2Cl_2): δ = 8.18 (s, 1 H, N=CH), 8.17–8.11 (t, J = 8.0 Hz, 1 H, $4_{pyridine\text{-}H}$), 7.92–7.89 (d, J = 7.5 Hz, 1 H, pyridine), 7.64–7.61 (d, J = 7.9 Hz, 1 H, pyridine), 7.38–7.32 (t, J = 7.2 Hz, 1 H, p-CH-C_6H_3), 7.22–7.18 (d, J = 8.0 Hz, 2 H, 2 × m-CH-C_6H_3), 7.06 (s, 2 H, C_6H_2), 3.40–3.28 [sept, J = 6.8 Hz, 2 H, 2 × CH(CH_3)$_2$], 3.02–2.88 [sept, J = 7.0 Hz, 1 H, p-CH(CH_3)$_2$], 2.62–2.50 [sept, J = 6.8 Hz, 2 H, 2 × CH(CH_3)$_2$], 1.59–1.56 (d, J = 6.8 Hz, 6 H, 2 × CH_3), 1.37–1.36 (d, J = 6.8 Hz, 6 H, 2 × CH_3), 1.29–1.26 (d, J = 6.9 Hz, 6 H, 2 × CH_3), 1.18–1.15 (d, J = 6.9 Hz, 6 H, 2 × CH_3), 1.10–1.08 (d, J = 6.8 Hz, 6 H, 2 × CH_3) ppm. ^{13}C NMR (62.90 MHz, CD_2Cl_2): δ = 170.22 (N=CH), 166.71, 154.88, 151.11, 146.18, 143.42, 141.13, 139.20, 134.39, 134.16, 128.90, 127.70, 123.70, 121.24, 34.74, 31.72, 29.07, 25.18, 24.53, 24.18, 24.11, 23.18 ppm. $C_{33}H_{44}Cl_2N_2Pd{\cdot}C_4H_8O$ (718.15): calcd. C 61.88, H 7.30, N 3.90; found C 61.40, H 7.33, N 3.61.

10: Compound **3b** (0.24 g, 0.512 mmol), [$NiCl_2$(dme)] (0.113 g, 0.512 mmol), and thf (50 mL) were added together in a Schlenk flask under an atmosphere of nitrogen. The reaction mixture was stirred at 70 °C for 18 h. The solvent was removed, and the beige precipitate was washed with hexane, dissolved in thf, and filtered through quartz. After concentration, beige crystals were grown at –25 °C and dried under vacuum. Yield: 0.044 g (15%). μ_{eff} = 2.57 BM (26 °C). ^{1}H NMR (250.13 MHz, $CDCl_3$): δ = 39.53, 24.43, 17.49, 11.24, 5.51, 3.46, 2.78, 2.53, 2.16, 1.25, 1.17, 1.14, 0.03, –4.63 ppm. $C_{33}H_{44}Cl_2N_2Ni$ (598.32): calcd. C 66.24, H 7.41, N 4.68; found C 65.94, H 7.22, N 4.44.

11: Compound **3b** (0.283 g, 0.604 mmol) and $CoCl_2$ (0.08 g, 0.604 mmol) were dissolved in thf (40 mL). The resulting dark green reaction mixture was stirred for 20 h at 60 °C. The solvent was removed under vacuum. The product was washed with hexane, dissolved in thf, filtered through quartz, and concentrated. Green crystals were collected at –25 °C. Yield: 0.21 g (58%). M.p. 272 °C. μ_{eff} = 4.38 BM (26 °C). ^{1}H NMR (250.13 MHz, $CDCl_3$): δ = 28.16, 21.32, 8.29, 8.20, 7.86, 7.12, 7.07, 6.88, 5.05, 3.72, 3.11, 2.93, 2.50, 1.62, 1.39, 1.23, 1.12, 0.82, 0.70, 0.35, 0.04, –1.56, –4.38, –5.26, –5.43 ppm. $C_{33}H_{44}Cl_2CoN_2$ (598.56): calcd. C 66.22, H 7.41, N 4.68; found C 65.89, H 7.62, N 4.51.

Acknowledgments

Financial support from the Fonds der Chemischen Industrie is gratefully acknowledged.

[1] S. Mecking, *Angew. Chem.* **2001**, *113*, 550–557; *Angew. Chem. Int. Ed.* **2001**, *40*, 534–540.

[2] a) G. J. P. Britovsek, V. C. Gibson, D. F. Wass, *Angew. Chem.* **1999**, *111*, 448–468; *Angew. Chem. Int. Ed.* **1999**, *38*, 428–447; b) S. D. Ittel, L. K. Johnson, M. Brookhart, *Chem. Rev.* **2000**, *100*, 1169–1203; c) C. Bianchini, G. Mantovani, A. Meli, F. Migliacci, F. Zanobini, F. Laschi, A. Sommazzi, *Eur. J. Inorg. Chem.* **2003**, 1620–1631.

[3] a) D. M. Haddleton, C. B. Jasieczek, M. J. Hannon, A. J. Shooter, *Macromolecules* **1997**, *30*, 2190–2193; b) P.-L. Bres, V. C. Gibson, C. D. F. Mabille, W. Reed, D. F. Wass, R. H. Weatherhead, *WO 98/49208* **1998**; c) D. M. Haddleton, D. J. Duncalf, D. Kukulj, M. C. Crossman, S. G. Jackson, S. A. F. Bon, A. J. Clark, A. J. Shooter, *Eur. J. Inorg. Chem.* **1998**, 1799–1806; d) G. M. DiRenzo, M. Messerschmidt, R. Mülhaupt, *Macromol. Rapid Commun.* **1998**, *19*, 381–384; e) A. J. Amass, C. A. Wyres, E. Colclough, I. M. Hohn, *Polymer* **2000**, *41*, 1697–1702; f) V. C. Gibson, R. K. O'Reilly, D. F. Wass, A. J. P. White, D. J. Williams, *Dalton Trans.* **2003**, 2824–2830.

[4] a) C. Bianchini, A. Sommazzi, G. Mantovani, R. Santi, F. Masi, *WO 02/34701 A1* **2002**; b) C. Bianchini, G. Mantovani, A. Meli, F. Migliacci, F. Laschi, *Organometallics* **2003**, *22*, 2545–2547; c) C. Bianchini, G. Giambastiani, G. Mantovani, A. Meli, D. Mimeau, *J. Organomet. Chem.* **2004**, *689*, 1356–1361; d) C. Bianchini, G. Giambastiani, A. Meli, A. Toti, *Organometallics* **2007**, *26*, 1303–1305; e) C. Bianchini, D. Gatteschi, G. Giambastiani, R. Guerrero Rios, A. Lenco, F. Laschi, C. Mealli, A. Meli, L. Sorace, A. Toti, F. Vizza, *Organometallics* **2007**, *26*, 726–739.

[5] a) R. Chen, S. F. Mapolie, *J. Mol. Catal. A* **2003**, *193*, 33–40; G. S. Smith, S. F. Mapolie, *J. Mol. Catal. A* **2004**, *213*, 187–192; R. Chen, J. Bacsa, S. F. Mapolie, *Polyhedron* **2003**, *22*, 2855–2861; J. Cloete, S. F. Mapolie, *J. Mol. Catal. A* **2006**, *243*, 221–225.

[6] Suzuki cross-coupling reactions involving sterically demanding substrates: a) N. G. Andersen, S. P. Maddaford, B. A. Keay, *J. Org. Chem.* **1996**, *61*, 9556–9559; b) M. G. Johnson, R. J. Foglesong, *Tetrahedron Lett.* **1997**, *38*, 7001–7002; c) J. Yin, S. L. Buchwald, *J. Am. Chem. Soc.* **2000**, *122*, 12051–12052; d) A. N. Cammidge, K. V. L. Crépy, *Chem. Commun.* **2000**, 1723–1724; e) A.-S. Castanet, F. Colobert, P.-E. Broutin, M. Obringer, *Tetrahedron: Asymmetry* **2002**, *13*, 659–665; f) R. B. Bedford, S. L. Hazelwood, M. E. Limmert, J. M. Brown, S. Ramdeehul, A. R. Cowley, S. J. Coles, M. B. Hursthouse, *Organometallics* **2003**, *22*, 1364–1371; g) R. B. Bedford, C. S. J. Cazin, M. B. Hursthouse, M. E. Light, V. J. M. Scordia, *Dalton Trans.* **2004**, 3864–3868; h) A. N. Cammidge, K. V. L. Crépy,

Tetrahedron **2004**, *60*, 4377–4386; i) P.-E. Broutin, F. Colobert, *Eur. J. Org. Chem.* **2005**, 1113–1128; j) H. Li, Y. Wu, W. Yan, *J. Organomet. Chem.* **2006**, *691*, 5688–5696.

[7] N. M. Scott, T. Schareina, O. Tok, R. Kempe, *Eur. J. Inorg. Chem.* **2004**, 3297–3304.

[8] a) N. M. Scott, R. Kempe, *Eur. J. Inorg. Chem.* **2005**, 1319–1324; b) W. P. Kretschmer, A. Meetsma, B. Hessen, T. Schmalz, S. Qayyum, R. Kempe, *Chem. Eur. J.* **2006**, *12*, 8969–8978; c) W. P. Kretschmer, A. Meetsma, B. Hessen, N. M. Scott, S. Qayyum, R. Kempe, *Z. Anorg. Allg. Chem.* **2006**, *632*, 1936–1938.

[9] For a review on aminopyridinato ligands, see: R. Kempe, *Eur. J. Inorg. Chem.* **2003**, 791–803.

[10] H. Maisel, S. Keller, T. Irrgang, R. Kempe, *Z. Kristallogr. New Cryst. Struct.* **2005**, *220*, 463–464.

[11] a) G. Bähr, H. Thämlitz, *Z. Anorg. Allg. Chem.* **1955**, *282*, 3; b) G. Bähr, H. G. Döge, *Z. Anorg. Allg. Chem.* **1957**, *292*, 19; c) G. Schmauss, P. Barth, *Z. Naturforsch. Teil B* **1970**, *25*, 789; d) M. E. Cucciolito, V. De Felice, A. Panunzi, A. Vitagliano, *Organometallics* **1989**, *8*, 1180–1187; e) S. Plentz Meneghetti, P. J. Lutz, J. Kress, *Organometallics* **1999**, *18*, 2734–2737; f) T. V. Laine, M. Klinga, M. Leskelä, *Eur. J. Inorg. Chem.* **1999**, 959–964; g) T. V. Laine, K. Lappalainen, J. Liimatta, E. Aitola, B. Löfgren, M. Leskelä, *Macromol. Rapid Commun.* **1999**, *20*, 487–491; h) T. V. Laine, M. Klinga, A. Maaninen, M. Leskelä, *Acta Chem. Scand.* **1999**, *53*, 968; i) T. V. Laine, U. Piironen, K. Lappalainen, M. Klinga, E. Aitola, M. Leskelä, *J. Organomet. Chem.* **2000**, *606*, 112–124; j) C. Bianchini, H. M. Lee, G. Mantovani, A. Meli, W. Oberhauser, *New J. Chem.* **2002**, *26*, 387–397.

[12] For selected examples of Grignard coupling reactions efficiently catalyzed by iron compounds, see: a) F. Babudri, A. D'Ettole, V. Fiandanese, G. Marchese, F. Naso, *J. Org. Chem.* **1991**, *405*, 53–58; b) A. Fürstner, A. Leitner, M. Méndez, H. Krause, *J. Am. Chem. Soc.* **2002**, *124*, 13856–13863; c) T. Nagano, T. Hayashi, *Org. Lett.* **2004**, *6*, 1297–1299; d) M. Nakamura, K. Matsuo, S. Ito, E. Nakamura, *J. Am. Chem. Soc.* **2004**, *126*, 3686–3687; e) B. Scheiper, M. Bonnekessel, H. Krause, A. Fürstner, *J. Org. Chem.* **2004**, *69*, 3943–3949; f) K. Itami, S. Higashi, M. Mineno, J.-I. Yoshida, *Org. Lett.* **2005**, *7*, 1219–1222; g) R. B. Bedford, M. Betham, D. W. Bruce, A. A. Danopoulos, R. M. Frost, M. Hird, *J. Org. Chem.* **2006**, *71*, 1104–1110.

[13] H. Maisel, S. Keller, T. Irrgang, R. Kempe, *Z. Kristallogr. New Cryst. Struct.* **2005**, *220*, 465–466.

[14] F. A. Cotton, R. L. Luck, Kyung-ae Son, *Acta Crystallogr. Sect. C: Cryst. Struct. Commun.* **1990**, *46*, 1424–1426.

[15] Z. Janas, P. Sobota, T. Lis, *J. Chem. Soc. Dalton Trans.* **1991**, 2429–2434.

[16] A. Altomare, M. C. Burla, M. Camalli, G. L. Cascarano, C. Giacovazzo, A. Guagliardi, A. G. G. Moliterni, G. Polidori, R. Spagna, *J. Appl. Crystallogr.* **1999**, *32*, 115–119.

[17] G. M. Sheldrick, *SHELXL-97: Program for Crystal Structure Analysis* (Release 97–2), Institut für Anorganische Chemie der Universität, Göttingen, Germany, **1998**.

[18] L. J. Farrugia, *J. Appl. Crystallogr.* **1999**, *32*, 837–838.

Received: April 12, 2007
Published Online: July 18, 2007

